SECOND EUROPEAN CONFERENCE ON EARTHQUAKE ENGINEERING
AND SEISMOLOGY, ISTANBUL AUG. 25-29, 2014

EFFECT OF REINFORCEMENT DETAILING IN THE SEISMIC BEHAVIOR OF SLENDER WALLS

Matías A. HUBE[1], Andrés MARIHUEN[2] and Juan Carlos DE LA LLERA[3]

ABSTRACT

Significant damage was observed in reinforced concrete walls of residential buildings following the 2010 Maule earthquake in Chile. The damage in structural walls was brittle and concentrated near the ground level. The most common observed damage in such walls was crushing of concrete under flexural-compressive action, buckling and fracture of the vertical reinforcement, and opening of horizontal reinforcement. This damage is attributed to high axial loads, the limited wall thickness, the inadequate reinforcement detailing, and structural irregularities. The objective of this paper is to summarize the experimental campaign of four 1/2-scale reinforced concrete walls (W1, W7, W8 and W9). The tests are aimed to assess the influence of the horizontal reinforcement detailing in the seismic behaviour of slender walls. Wall specimen W1 is referred to as the reference wall and was designed following typical construction practice in Chile, with the horizontal bars bent with 90-degreee hook. Specimen W7 was designed with horizontal bars bent with 135-degree hooks, specimen W8 with additional closed stirrups in the wall boundaries, and specimen W9 with additional transverse cross-ties. The aspect ratio of the walls was M/Vl_w=2.5, and the thickness of the scaled specimens was 100 mm. The walls were subjected to a constant axial load of $0.15f_c^{'}A_g$ and were subjected to lateral cyclic displacements. It is concluded that the 135-degree hooks does not improve significantly the behaviour of slender walls. The use of closed stirrups at the wall boundaries are highly recommended to reduce the likelihood of bar buckling, as well as to prevent out-of-plane buckling of the wall after failure.

INTRODUCTION

The 2010 Maule earthquake affected more than 12 million people, which represents about 70% of Chile's population. A tsunami was triggered due to the earthquake and about 560 people died mostly due to the tsunami. More than 80,000 residences were destroyed, approximately 300 bridges were damaged (Buckle et al. 2012), and about 40 reinforced concrete (RC) buildings with nine or more stories was severely damage (Wallace et al. 2012). These damaged buildings corresponded to about 2% of the buildings with nine or mores stories in south Central Chile.

Chilean buildings are characterized by having a large number of RC walls to resist both gravity and lateral forces. They are structured with larger walls in the longitudinal direction of the buildings and shorter walls in the transverse direction (Jünemann et al. 2012). The cross sections of the transverse walls are often T-shape or L-shape and the total wall area to floor plan area is about 3% on

[1]Assistant Professor, Pontificia Universidad Católica de Chile and National Reserach Center of Integrated Natural Disaster Management CONICYT/FONDAP/1510017, Santiago, Chile, mhube@ing.puc.cl
[2] Graduate Student,Pontificia Universidad Católica de Chile, Santiago, Chile, andresmarihuen@gmail.com
[3] Professor, Pontificia Universidad Católica de Chile, Chile and National Reserach Center of Integrated Natural Disaster Management CONICYT/FONDAP/1510017, Santiago, Chile, Chile, jcllera@ing.puc.cl

each direction (Massone et al. 2012). Wall thickness of 15 cm and 20 cm are usual in construction practice and most walls were designed without special boundary reinforcement. Special boundary reinforcement was not required by NCh433 (INN 1996) because of the good performance of Chilean buildings after 1985 earthquake. The spacing of the horizontal web reinforcement is commonly 20 cm, and the ratio between the spacing of the horizontal web reinforcement and the diameter of the longitudinal boundary bar range from s/d_b =8 to 11 (Wallace et al. 2012). Typical detailing's of the horizontal web reinforcement are shown in Fig. 1. In Fig. 1a, the horizontal web reinforcement of each side of the wall is bent with 180-degree hook outside the vertical bars. On the other hand, in Fig. 1b one horizontal web reinforcement is bent with 180-degree hook and the other with 90-degree hook. In both detailing cases, the hooks are not anchored into the concrete core.

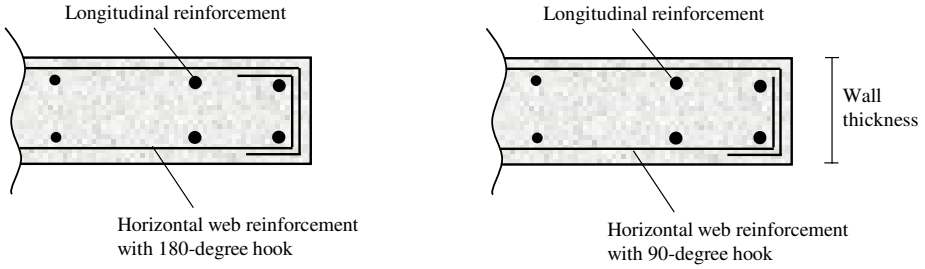

Figure 1. Typical detailing of horizontal web reinforcement in walls

Most of damaged buildings during the Maule earthquake were constructed after the year 2000 (Jünemann et al. 2012), and the observed damage was different than that observed after 1985 earthquake (Wood 1991). The most common observed damage during the Maule earthquake was crushing of concrete under flexural-compressive action, buckling and fracture of the vertical reinforcement, and opening of horizontal reinforcement. Example of the observed damage in walls is shown in Fig. 2. The damage in walls was attributed to high axial loads, the limited wall thickness, the inadequate reinforcement detailing, and structural irregularities (Wallace et al. 2012, Westenenk et al. 2013). The large spacing of the horizontal web reinforcement, and the opening of the 90-degree hook of the horizontal reinforcement after concrete spalling likely contributed to buckling of vertical reinforcement (Wallace et al. 2012).

Figure 2. Example of damaged walls due to 2010 Maule earthquake

After the Maule earthquake, several modifications were introduced in the Chilean design code (DS 60 2010; Massone 2013). A limit for the ultimate axial loads of walls of $0.35 f_c^{'} A_g$ was introduced, where $f_c^{'}$ is the characteristic concrete strength, and A_g is the gross cross-section area. To control the

wall thickness, the lateral wall instability has to be considered in design if the story height to wall thickness ratio is larger than 16. Additionally, new requirements for special boundary renforcement were incorporated. Similarly to ACI 318 (2008), special boundary reinforcement is required in walls if the concrete compressive strain demand is larger than 0.003. The compressive strain demand is estimated from the building design roof displacement (δ_u). The compressive strain demand in the most compressed fiber at the critical section is limited to 0.008, which is not the case of ACI 318.

The objective of this paper is to study the effect of the horizontal reinforcement detailing in the seismic behaviour of slender walls. To achieve this objective, the experimental results of four ½-scale wall specimens are summarized and discussed in this paper. The detailing of the horizontal reinforcement of the reference wall was designed following typical construction practice in Chile at the time of the earthquake (Fig. 1). The other three walls were designed with different horizontal reinforcement detailing aimed to improve the seismic behaviour.

EXPERIMENTAL PROGRAM

A total of nine ½-scale wall specimens (W1 to W9) were constructed and tested in a larger research program conducted at Pontificia Universidad Catolica de Chile (Hube et al. 2014). These walls specimens were tested to understand and reproduce experimentally the damage observed in walls after the Maule earthquake. Additionally, they were tested to analyse the effect of the axial load, wall thickness, aspect ratio, and reinforcement detailing on the seismic behaviour of walls.

This paper summarizes the experimental results of four walls (W1, W7, W8 and W9), which were constructed with different horizontal reinforcement detailing. The effect of axial loads was obtained from wall specimens W1, W2, and W3, and is discussed elsewhere (Alarcon et al. 2014). The test matrix of the walls discussed in this paper is shown in Table 1, were wall W1 is the reference wall of the experimental program. These four walls were tested with a constant axial load of $N = 0.15 f_c' A_g = 287$ kN, and were subected to lateral cyclic displacements.

Table 1. Test Matrix

Wall Specimen	Test Purpose
W1	Reference wall
W7	Horizontal reinforcement detailing effect
W8	Boundary confinement effect
W9	Cross-ties effect

The characteristics of the reference wall W1 were defined based on the characteristics of critical walls of five damaged RC buildings (Alarcon et al. 2014). The wall thickness of these critical walls varied from 150 mm to 250 mm, and 200 mm was selected for the prototype wall (100 mm thickness for the ½-scale specimen). The average ALR for service gravity load of the critical walls was 0.18, and 0.15 was selected as the ALR of the reference wall, where $ALR = N / f_c' A_g$ .The average aspect ratio M/Vl_w of the damaged walls was 2.02 and a ratio of 2.5 was selected for the reference wall to ensure a flexural mode of failure. The reinforcement ratios of the longitudinal boundary reinforcement, uniformly distributed vertical reinforcement, and horizontal web reinforcement of the reference wall, were selected from the average ratios of the critical walls of the five damaged buildings (Alarcon et al. 2014).

The dimensions and reinforcement detailing of the reference wall W1 are shown in Fig. 3. The dimension of this wall specimen is identical to walls W7, W8 and W9. The length of the wall is 700 mm, the thickness 100 mm, and the height 1600 mm. The walls were cast with a 425 x 400 x 1400 mm RC base to anchor them to the laboratory strong floor, and with a 300 x 300 x 700 mm top RC beam to apply the vertical and lateral loads. Wall W1 is reinforced with four ϕ10 (10 mm diameter) longitudinal boundary bars and six ϕ8 mm bars in two layers as uniformly distributed vertical reinforcement. The horizontal web reinforcement consists on ϕ5 mm bars in two layers and spaced at 90 mm. The resulting s/d_b ratio of wall W1, considering the longitudinal boundary bars, is 9.

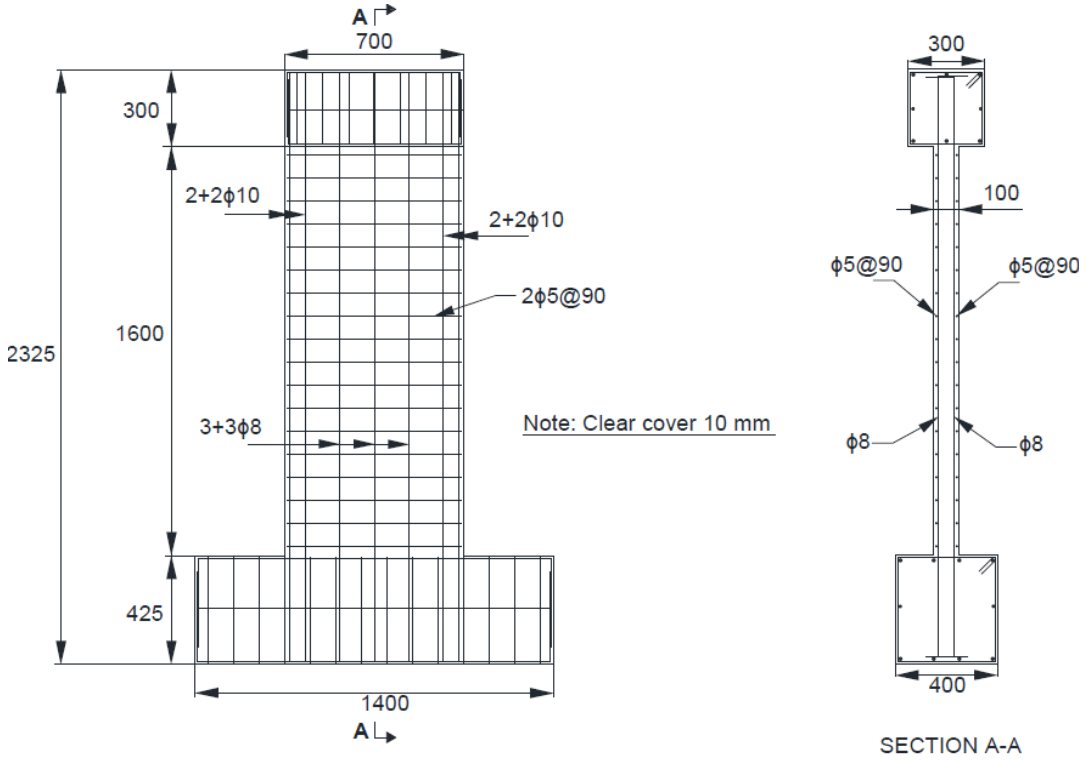

Figure 3. Dimensions and detailing of wall specimen W1

The cross section detailing of the four walls are shown in Fig. 4. The only difference of these walls is the detailing of the horizontal reinforcement. The detailing of the horizontal reinforcement of wall specimen W1 (Fig. 4a) follows typical construction practice, with 90-degree hooks bent outside the vertical bars (Fig. 1b). These horizontal bars are not anchored into the concrete core and become ineffective after spalling of concrete cover (Wallace et al. 2012). The opening of the horizontal reinforcement in a damaged wall can be observed in the right photograph in Fig. 2. Wall W7 was designed with the horizontal web reinforcement bent with 135-degree hooks (Fig. 3b) to assess the effect of anchoring the horizontal reinforcement in the concrete core of slender walls. Wall W8 was designed with the same horizontal reinforcement as W1, but with additional closed stirrups spaced at 90 mm at the wall boundary (Fig. 3c). The stirrups were placed in the middle of the layers of the horizontal web reinforcement and the resulting s/d_b ratio of the longitudinal boundary bars is 4.5. Finally, wall W9 was designed with the same horizontal reinforcement as W1, but with additional cross-ties on every longitudinal bar at each level of horizontal reinforcement (except, for the outermost boundary bars), Fig. 4d.

The concrete compressive strength was f_c' = 27.4 MPa. This strength was measured using standard cylinder samples that were tested one day before the first wall test at an age of 160 days. The measured secant modulus of elasticity at $0.4 f_c'$ was E_c = 32,700 Mpa. The properties of the reinforcing steel are summarized in Table 2.

The test setup is shown in Fig. 5. The walls were bolted to the strong floor and were connected with a pin at the top. The horizontal 500 kN actuator was pinned at both ends and was attached to the top RC beam of the walls with four steel bars that were bolted against a steel plate at each side of the wall. The effective height from the base of the wall to the horizontal actuator axis was 1750 mm, which result in an aspect ratio of M/Vl_w = 2.5. A 5kN counterweight was connected to the clevis of the horizontal actuator at the wall side using two pulleys. This counterweight (not shown in Fig. 5) was used to hang the actuator and eliminate the bending moment in the wall induced by the weight of the actuator. The 700 kN vertical actuator was bolted at the top to the steel frame. This actuator was connected to the wall using a clevis that was connected to a steel plate with rollers, which allowed the

horizontal displacement of the wall. Therefore, the P-delta effect was not included in the test setup. The out-of-plane displacement of the walls was restrained with rolling supports that were connected to a steel I-beam at each side of the top beam (Fig. 5).

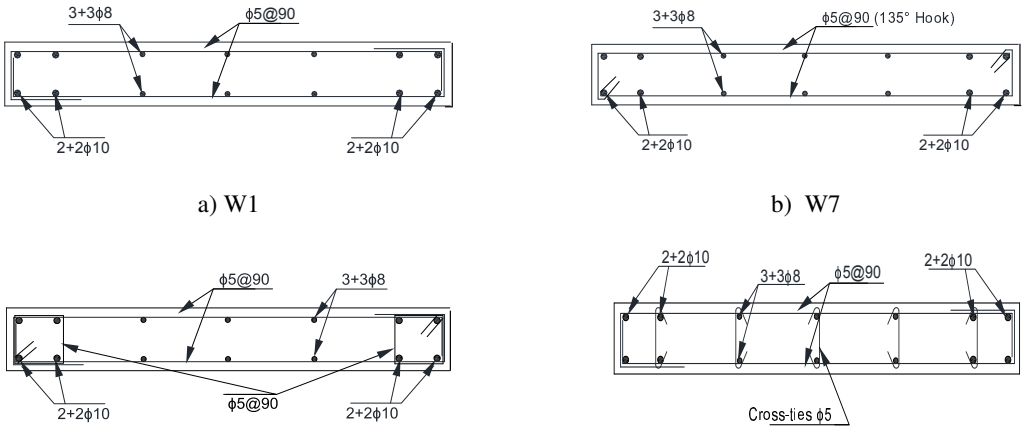

Figure 4. Reinforcement detailing of wall specimens

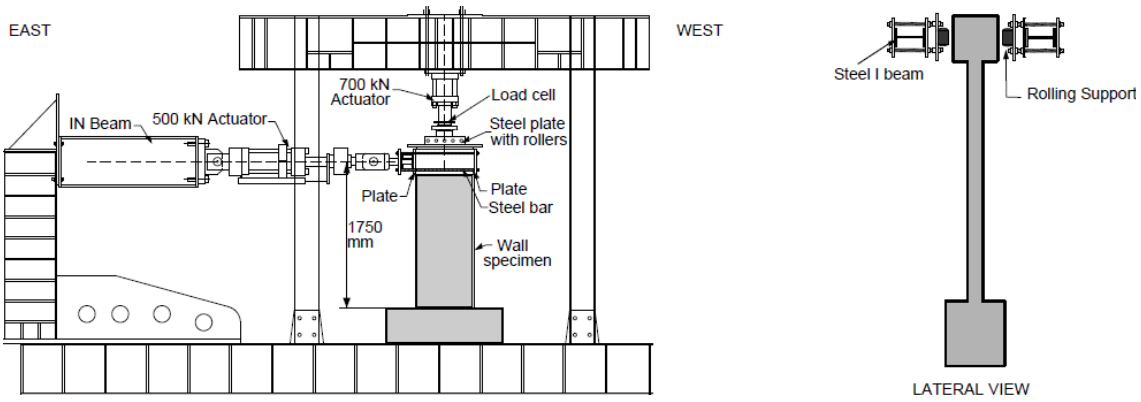

Figure 5. Test setup (lateral view shown with larger scale)

Table 2. Average properties of reinforcing steel

Parameter	ϕ5	ϕ8	ϕ10
Steel	AT560-500H	A630-420H	A630-420H
Yield strength (MPa)	608.9	445.6	469.2
Ultimate strength (MPa)	667.7	598.9	675.7
Modulus of elasticity (GPa)	-	225.8	224.7
Yield strain	-	0.0020	0.0021
Hardening strain	-	0.0139	0.0138
Ultimate strain	0.057	0.151	0.166
Strain Hardening modulus (MPa)	-	4130	5430

Each wall was instrumented with 2 load cells, 14 displacement transducers and 16 strain gauges attached to the reinforcement, Fig. 6. Additionally, the deformations of each wall were measured with a high resolution camera using the digital image correlation method. Load cells were connected to both horizontal and vertical actuators in order to measure the applied loads. The displacement

transducers were installed to measure walls displacement and to obtain curvatures. The strain gauges were used to measure the strain in several reinforcing bars and were installed during the construction process of the walls.

The four specimens were subjected to a constant ALR of 0.15 and increasing lateral displacements. Following the application of the vertical load, the specimens were subjected to horizontal displacement with increasing amplitude and with two cycles at each amplitude. The displacement cycles were designed based on the horizontal yield displacement of the wall specimens which was estimate as Δ_y = 5.5 mm for specimen W1. The yield displacement was obained assuming a linear curvature distribution along the specimen height. The ductility factors (Δ/Δ_y) that were intended to be applied at peak displacements of the walls were 0.5, 1, 1.5, 2, 3, 4, 5, 6, and 8. The horizontal displacement was applied at a rate of 10 mm/min.

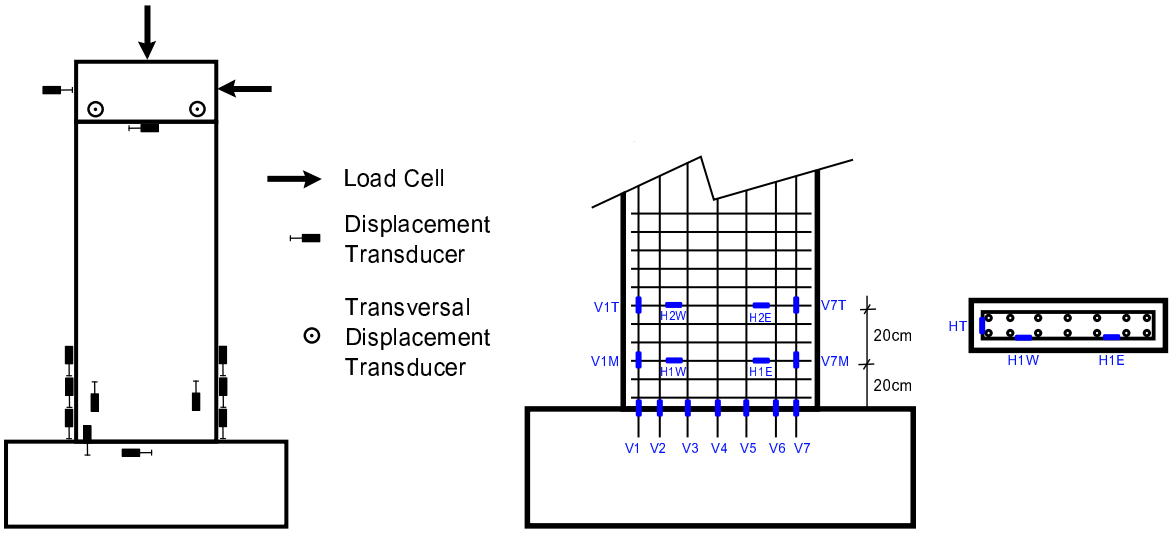

Figure 6. Instrumentation of wall specimens, 2 load cells, 16 displacement transducers and 16 strain gauges

TEST RESULTS

The behaviour and failure of the four wall specimens was controlled by flexural-compressive interactions due to the relatively high M/Vl_w ratio. The damage propagation of wall specimen W7 is shown in Fig. 7. The first cracks observed in the walls specimens were diagonal shear cracks along the height of the walls (Fig. 7a), which were followed by horizontal flexural cracks near the base of the walls. After several cycles, spalling cracks appeared at the bottom boundaries of the wall due to the compressive stresses induced by the axial load and bending moment (Fig. 7b). In subsequent cycles and in most specimens, buckling was observed in the outermost longitudinal boundary bars, and in the longitudinal boundary bars located in the second layer (Fig. 7c). Buckling of the longitudinal boundary bars was expected due to the high s/d_b ratio. Finally, a brittle compressive failure along the entire length of the walls was observed followed by an out-of-plane buckling in all but one of the tested wall (Wall W8). The front view of the four walls after failure is shown in Fig. 8, where damage was propagated throughout the entire wall length of the walls. The side view of the walls after failure is shown in Fig. 9. Damage in the four wall specimens was concentrated within a height that varied from $2.6t_w$ for wall specimen W7 to $4.3t_w$ for wall specimen W9. This height is slightly larger than the height between t_w and $3t_w$ of the damaged region in walls after the 2010 Maule earthquake reported by Wallace et al. (2012). Contrary to what was observed in walls damaged by the Maule earthquake, the longitudinal reinforcement in the four wall specimens did not fracture during the tests. The fracture of longitudinal bars in damaged buildings may be attributed to additional cycles in walls caused by the long duration of the earthquake. Since a constant vertical load was applied to the wall specimens, the

walls were not able to transfer this load to adjacent structural elements, and the wall specimens crushed in compression before any fracture of longitudinal reinforcement could develop.

Because of the 90-degree hook of the horizontal web reinforcement of wall specimen W1, the horizontal reinforcement opened up, as shown in Fig. 9a. This reinforcement opening was similar to that observed in damaged walls after 2010 Maule earthquake (Fig. 2). On the other hand, the horizontal web reinforcement of wall W7 opened less than that of wall W1 because of the 135-degree hook. Nevertheless, due to the loss of concrete caused by concrete crushing and spalling, the 135-degree hook became visible, Fig. 9b.

The use of closed boundary stirrups in wall specimen W8 was effective to reduce the likelihood of bar buckling of the longitudinal boundary bars (Fig. 8c, Fig. 9c). This result was anticipated because the s/d_b ratio was reduced from 9 in wall W1 to 4.5 in wall W8. Bar buckling of the uniformly distributed vertical bars was observed in wall W8, but only after the compressive failure of the wall (Fig. 8c). An additional relevant result was observed in the failure mode of wall W8. After the compressive failure of concrete, a limited out-of-plane buckling was observed in wall W8 whereas, whereas a more severe out-of-plane buckling was observed in all other tested walls. Fig. 9c shows the east boundary of wall specimen W8 which did not buckle after failure. However, the west boundary of this wall suffered a limited out-of-plane buckling. The restrain of the out-of-plane buckling in wall specimen W8 is attributed to the confined RC boundary columns that restrained the out-of-plane displacement after the failure. This failure mode with a limited out-of-plane buckling is desirable in slender walls to maintain the capacity to resist vertical loads.

The observed damage in wall specimen W9, which was detailed with additional cross ties, was different than the observed damage in wall W8. Buckling of longitudinal boundary bars was not prevented in wall W9 because of the large s/d_b ratio (Fig. 8d). Eventhough every longitudinal bar was restrained with a cross-tie in wall W9, buckling was observed in these bars. However, the observed effective length of these bars was equal to the spacing of the horizontal web reinforcement (i.e. 90 mm), whereas the effective length of bars in wall W1 was larger than the spacing of the horizontal web reinforcement because of the lack of transverse restrain. Finally, the use of cross ties in wall W9 may have increased concrete confinement throughout the wall cross section.

a) Diagonal shear cracks (1.35% drift) b) Spalling cracks (1.73% drift) c) Buckling of longitudinal boundary bars (2.11% drift)

Figure 7. Damage propagation wall specimen W7

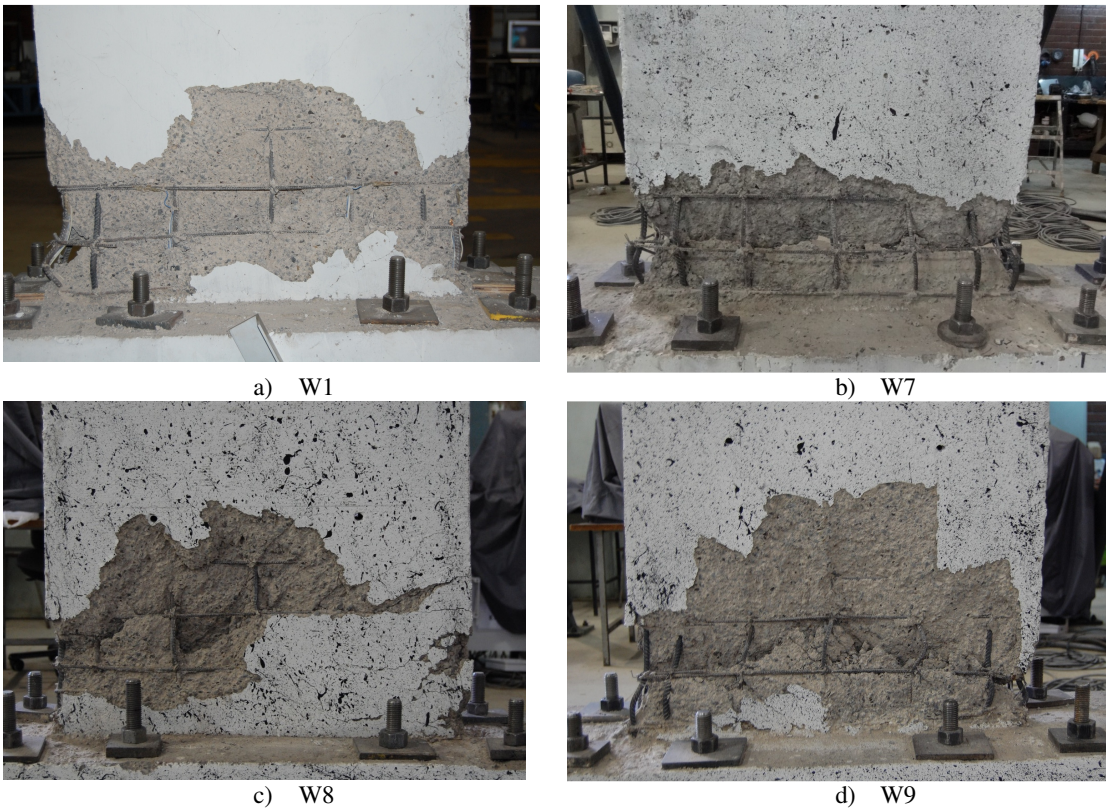

a) W1 b) W7

c) W8 d) W9

Figure 8. Front view of wall specimens after failure

a) W1 b) W7 c) W8 d) W9

Figure 9. Side view of wall specimens after failure

The localized damage observed in the tested wall specimens may not be related to bar buckling as suggested by Wallace et al. (2012). The height of the damaged region of wall specimen W1 was $3.6t_w$ and was comparable to the height of $3.7t_w$ of wall specimen W8, with smaller s/d_b ratio (Fig. 8). The largest damaged region, with a height of $4.3t_w$, was observed in wall specimen W9.

Therefore, the localized damage may be attributed to the limited thickness of the walls. After concrete spalling the cross section of the wall is reduced significantly, which may explain damage localizarion.

The lateral load displacement relationships and the moment curvature relationships of the four wall specimens are shown in Fig. 10 and Fig. 11, respectively. The summary of the test results are listed in Table 3. The curvature was obtained using the two displacement transducers installed at the bottom of the walls (Fig. 6), that measured the vertical displacement of two points separated at 150 mm in the wall edges. The moment was calculated using a lever arm equal to the distance between the wall base and the horizontal actuator axis (1750 mm), Fig. 5. The curvature of each test was not recorded until the end of each test because the instruments where removed after concrete spalling. The yield point in Table 3 was defined at the time step when yielding was first detected from the strain gauge measurements. The displacement ductility in Table 3 is estimated as the ratio between the ultimate displacement and the yield displacement. Since a lot of scatter was obtained for the experimental yield displacement, the analytical yield displacement of 55 mm (0.31%drift) was used to compute displacement ductility. Finally, the normalized dissipated energy in Table 3 is calculated as the ratio between the encircled are in the last completed cycle and the area of the enveloping rectangle in the load displacement relationship.

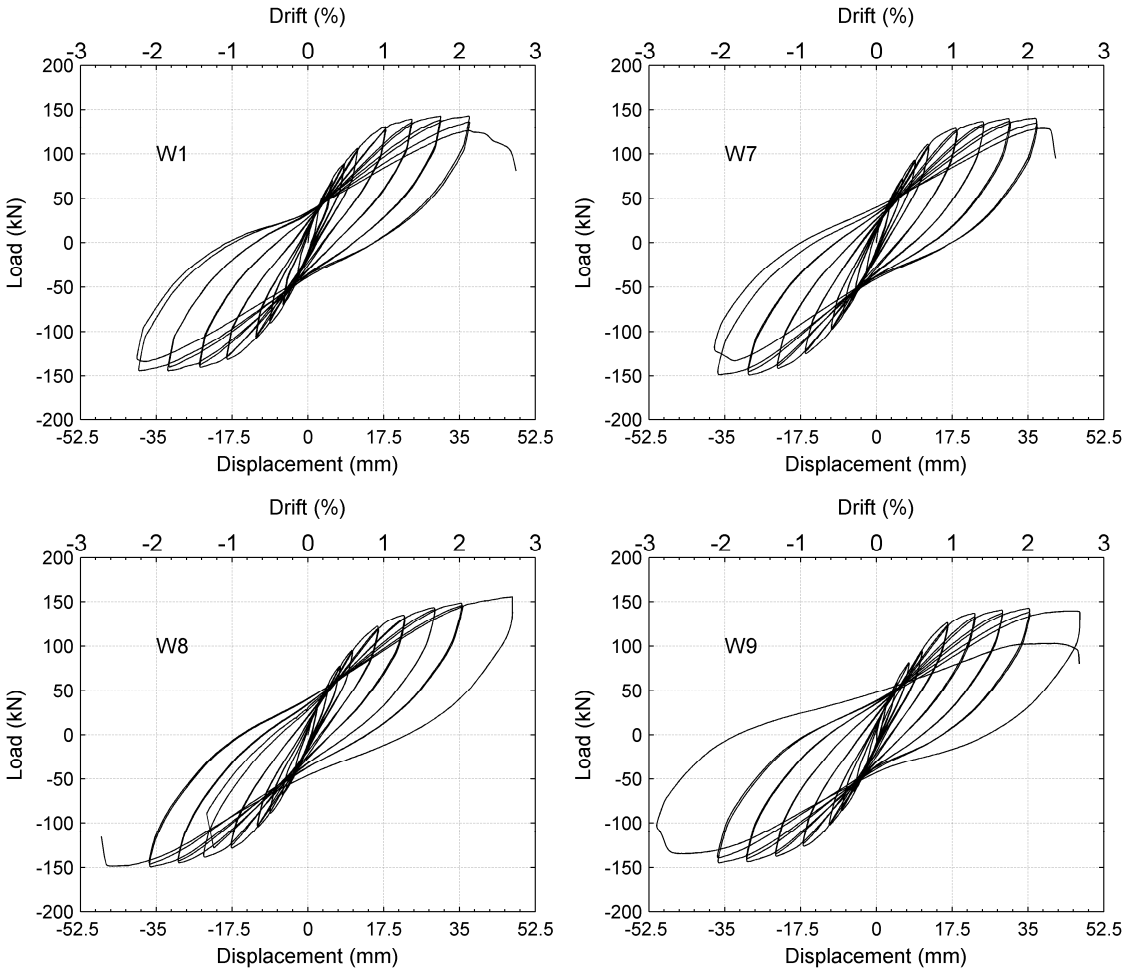

Figure 10. Load-displacement relationships

From Fig. 10 it can be observed that horizontal web reinforcement bent with 135-degree hooks of wall specimen W7 does not improve significantly the behavior compared of the wall, when comparing to wall specimen W1. Both walls failed at the first cycle with the target ductility factor of 8. In fact, the ultimate drift and the displacement ductility of wall W7 are 14% smaller and those of wall

W1. However the strength, and the dissipated normalized energy of wall W7 were 4%, and 7% larger than that of wall W1.

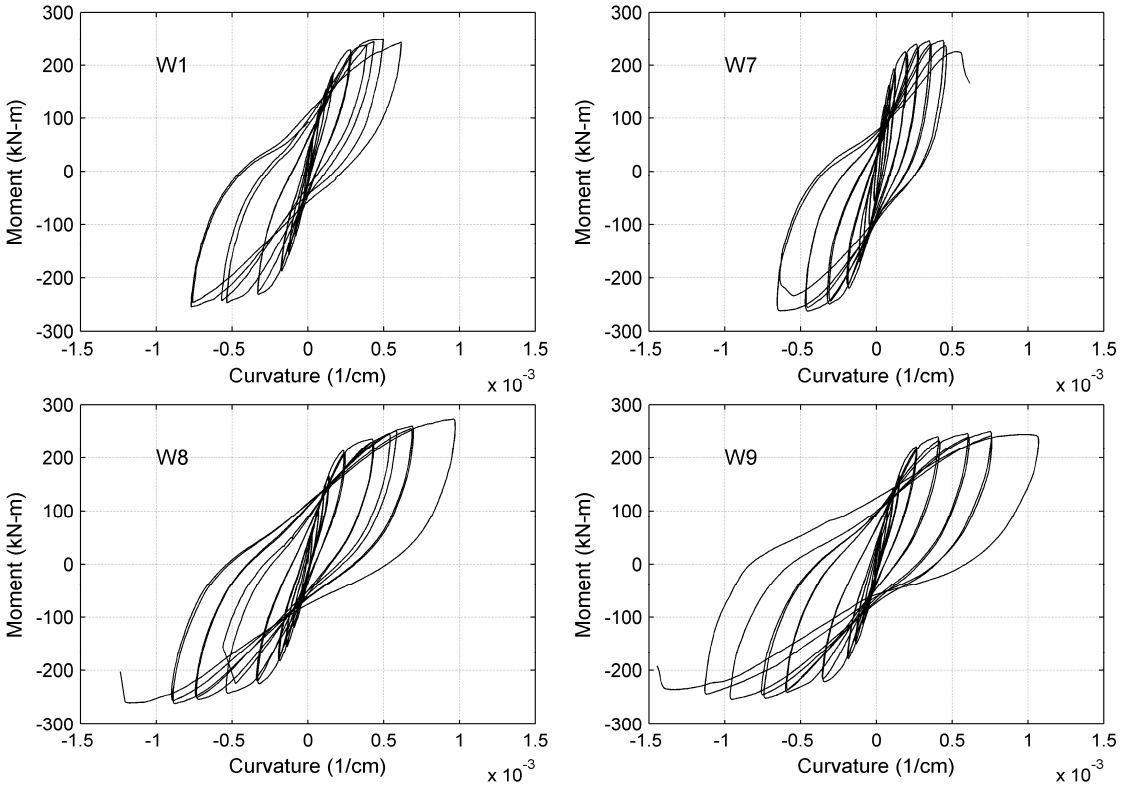

Figure 11. Moment-curvature relationships

Table 3. Summary of test results

Result	W1	W7	W8	W9
Yield load (kN)	92	76	81	74
Peak load (kN)	144	149	159	145
Drift at yielding (%)	0.55	0.36	0.42	0.34
Drift at ultimate displacement (%)	2.75	2.36	2.72	2.68
Displacement ductility (*)	8.9	7.6	8.8	8.6
Normalized dissipated energy	0.27	0.29	0.25	0.36

(*) The displacement ductility was obtained using the analytical yield displacement of 55 mm (0.31% drift)

The addition of closed stirrups between the layers of horizontal reinforcement in wall specimen W8 increases the strength by 8% when compared to wall W1 (Table 3). The ultimate drift and displacement ductility of wall specimen W8 are comparable to that of wall W1, but wall W8 was able to resist the first peak at the cycles with target ductility factor of 8 (2.7% drift in wall W8), which was not the case for W1 (Fig. 9). The use of closed stirrups also reduced the strength degradation in subsequent cycles of the same amplitude (Fig. 9). For the cycles with target ductility factors of 6, 2% strength degradation was measured in wall W8 whereas a 6% strength degradation was measured in wall W1. The strength degradation of wall specimen W1 was similar to that of wall specimen W7 with 135-degree hook. The larger strength degradation measured in wall specimens W1 and W7 may be explained by buckling of the longitudinal bars that occurred in the first cycles at that displacement amplitude. The smaller s/d_b ratio in wall specimen W8 restrained bar buckling and the measured strength degradation was smaller.

The addition of transverse cross ties in wall specimen W9 increased the normalized dissipated energy by and 33%, when comparing with wall W1. The ultimate drift and displacement ductility of wall specimen W9 are comparable to that of wall W1. However, wall W9 was the wall that resisted more cycles. Wall W9 was the only wall capable to resist the first two peaks at the cycles with target ductility factor of 8, and failed at the third peak with that amplitude (Fig. 9). The out-of-plane buckling was not prevented and the strength did not increased in wall W9 as it did in wall W8 because the s/d_b in wall W9 remained constant, and the longitudinal reinforcement evidenced buckling. The measured strength degradation in subsequent cycles with target ductility factors of 6 was 4%. This strength degradation in wall specimen W9 was smaller than that of wall W1 because the cross-ties in wall W9 restrained bar buckling of intermediate longitudinal bars. In fact, the effective length of longitudinal bars in wall W9 was smaller than the effective length of longitudinal bars in wall W1.

CONCLUSIONS

This paper summarizes the experimental campaign of four ½-scale walls that where tested to study the effect of the horizontal reinforcement detailing on the seismic behaviour of slender walls. The results of this experimental campaign may be used in future revision of the Chilean seismic code.

The tested walls responded predominantly in flexure due to the relatively high M/Vl_w ratio. The walls failed due to a compressive failure along the entire length of the wall base, followed by out-of-plane buckling in all but one the tested walls. The observed damage in the reference wall W1 was similar to that observed in structural RC walls in buildings damaged during the 2010 Maule earthquake.

It is concluded that the use of 135-degree hooks for the horizontal web reinforcement does not improve significantly the behaviour of the tested wall. The failure of wall specimen W7 occurred at the same peak amplitude cycle as that of wall specimen W1, even though, the horizontal reinforcement of wall W7 did not open up. The 135-degree hook was not that effective to improve the seismic behaviour in wall W7 may be due to the limited thickness of the walls, and the small amount of transverse reinforcement provided to confine the concrete core.

The use of closed stirrups at the wall boundaries in wall specimen W8 was effective to decrease the likelihood of longitudinal bar buckling, to decrease the strength degradation in subsequent cycles, and to limit the out-of-plane buckling of the wall specimen after failure. The failure mode of wall specimen W8, with a limited out-of-plane buckling, is a desirable failure mode in slender walls to maintain the capacity to resist vertical loads during an earthquake.

The use of cross-ties in wall specimen W9 increased the displacement capacity in the sense that wall specimen W9 was able to resist more displacement cycles than wall W1, although the drift at ultimate displacement was comparable to that of wall W1. The out-of-plane buckling of wall W9 was not prevented with the use of cross-ties.

AKNOWLEDGEMENTS

This study was financially supported by Chilean *Fondo Nacional de Ciencia y Tecnología*, Fondecyt through Grants #11121581, #1110377, and Fondap through Grant #15110017. The authors would also like to thank the graduate student C. Alarcón for his contribution in this project and the professors Bozidar Stojadinovic and Carl Lüders. The authors are also thankful to the engineers and technicians from DICTUC and the Laboratory of the Structural and Geotechnical Engineering Department of Pontifícia Universidad Católica de Chile.

REFERENCES

American Concrete Institute, ACI 318-08 (2008) "Building code requirements for structural concrete and commentary (318R-08)", Farmington Hills, MI, 465 pp.

Alarcon C, Hube MA, de la Llera JC (2014) "Effect of axial loads in the seismic behavior of reinforced concrete walls with unconfined wall boundaries," *Engineering Structures*, 73:13-23.

DS 60 MINVU (2010) "Reinforced concrete design code, replacing D.S N 118", Chilean Ministry of Housing and Urbanism, Diario Oficial, 13 December 2011 [in Spanish].

Buckle I, Hube M, Chen G, Yen W, Arias J (2012) "Structural performance of bridges in the offshore Maule earthquake of 27 February 2010," *Earthquake Spectra*, 28(S1):S533-S552.

Instituto Nacional de Normalización, INN (1996) "Earthquake resistant design of buildings, NCh433 Of96", Santiago, Chile, 41 pp (in spanish).

Jünemann R, Hube M, De La Llera JC, Kausel E (2012) "Characteristics of reinforced concrete shear wall buildings damaged during 2010 Chile earthquake", *Proceedings of the 15th World Conference of Earthquake Engineering*, Lisbon, Portugal, 24-28 September, Paper 2265.

Hube MA, Marihuén A, de la Llera JC, Stojadinovic B (2014) "Experimental campaign of reinforced concrete walls with non-seismic detailing," *Proceedings of the 10th U.S. National Conference on Earthquake Engineering*, Anchorage, Alaska, 21-25 July.

Massone L, Bonelli P, Lagos R, Lüders C, Moehle J, Wallace J (2012) "Seismic design and construction practices for RC structural wall buildings", *Earthquake Spectra*, 28(S1):S245-256.

Massone LM (2013) "Fundamental principles of the reinforced concrete design code changes in Chile following the Mw 8.8 earthquake in 2010," *Engingeering Structures*, 56:1335-1345.

Wallace J, Massone L, Bonelli P, Dragovich J, Lagos R, Lüders C, Moehle J (2012) "Damage and implications for seismic design of RC structural wall buildings," *Earthquake Spectra*, 28(S1):S281- S299.

Westenenk B, de la Llera JC, Jünemann R, Hube MA, Besa JJ, Lüders C, Inaudi JA, Riddell R, Jordán R (2013) "Analysis and interpretation of the seismic response of RC buildings in Concepción during the February 27, 2010, Chile earthquake", *Bulletin of Earthquake Engineering,* 11:69-91.

Wood SL (1991) "Performance of reinforced concrete buildings during the 1985 Chile earthquake: implications for the design of structural walls," *Earthquake Spectra* 7(4): 607-638.